SYNTHESIS, STABILITY, AND BANDGAP CONTROL FOR TWO-DIMENSIONAL SUPERLATTICES

CRISTIAN V. CIOBANU

Abstract. This article constitutes a brief review of recent results related to the experimental realization of one-dimensional interfaces between two-dimensional (2D) materials, along with their mechanical and electronic properties. In the current lore of 2D materials, the formation of spatially periodic domains of different materials constitutes a versatile way to enhance the range of electronic properties and phenomena that can be accessed for fundamental studies and technological applications. Mechanically, the domain boundaries are stable, but can become wrinkled or wavy under certain conditions. In terms of electronic properties, superlattices made of hybrid graphene and boron nitride domains can exhibit rich and spin-depedent behaviour: for example, they can be metallic in one spin component and semiconducting in the other, or semiconducting in both spin components with same or with different band gaps. The control parameters for accessing different electronic properties are the type of materials in the superlattices and their domain widths. These findings can be used in future generation electronic and spintronic devices based on 2D superlattices.

Key words: 2D materials, monolayer superlattices, domain boundaries.

1. INTRODUCTION

With the recent advances in controllable growth of large-area, high-quality, two-dimensional (2D) layered materials (e.g., graphene [1–4] and hexagonal boron nitride (hBN) [5, 6] on metallic substrates, the field has naturally progressed towards the design and/or investigation of heterostructures based on out-of-plane [7–11] or in-plane [12–14] stacking of these nanomaterials. Layered heterostructures of graphene and boron nitride offer the best avenue of preserving the exotic properties of graphene and using them in nanoscale devices, because of the near-perfect epitaxial lattice match, small van der Waals (vdW) interactions between graphene and hBN, and most importantly because of the insulating nature of the underlying hBN layer or layers.

Colorado School of Mines, Department of Mechanical Engineering, Golden, CO 80401, USA

Ro. J. Techn. Sci. – Appl. Mechanics, Vol. 61, N° 1, pp. 7–21 Bucharest, 2016

On the other hand, if a bandgap is necessary for certain applications and if close control of that bandgap over a wide range is desired for different purposes or applications, then in-plane heterostructures or arrangements of domains whose atomic type alternates in the plane may offer a good avenue for creating and controlling the bandgap and other electronic properties. New and stable 2D materials based on hybrid domains of spatially periodic arrangements (superlattices) thereof offer a way to make available a finer range of key electronic properties; the bandgap range in pure 2D materials is rather sparse at the moment, with graphene being semimetallic, hBN insulator with a gap of ~5 eV, and MoS_2 semiconducting with a gap of ~1.8 eV. The idea of bandgap control by exploiting the domain width as a control parameter come from the studies of nanoribbons of graphene [15], in which the bandgap appears due to the presence of nanoribbon edges; this bandgap varies with the width of the nanoribbon, and, moreover, it can be induced in one spin component and not in the other --a phenomenon commonly referred to half-metallicity [16]. Similar to graphene nanoribbons, hybrid domains form boundaries (instead of edges) separating the domains of each material (i.e., graphene or hBN). These domain boundaries are multiple and can repeat periodically in space, are not reactive (hence chemically stable), and are expected to produce novel electronic properties akin to those induced by the edges in graphene nanoribbons. Indeed, recent density functional theory (DFT) computations on graphene-hBN hybrid heterostructures have revealed half-metallicity in these 2D materials [17]. This is an important advance, since creating a bandgap in one spin component and not the other is the key to selective electronic transport based on spin (spintronics), which may lead to novel fundamental science and applications in terms of magnetic memories or storage, spin-based logic devices, and possibly others.

In this article, we present a brief review of the current state of the hybrid domains in terms of their synthesis and mechanical and electronic properties, which are presented in separate sections below. With excellent mechanical stability and exotic electronic properties, the bottleneck towards the large scale usage of these 2D nanomaterials is the lack of available large-scale synthesis techniques with reliable and controllable hybrid-domain dimensions. At the rate at which progress is achieved in 2D materials, it is reasonable to expect that this bottleneck will be overcome soon, as it can be inferred from very recent works on interface formation between graphene and hBN [12] and on using graphene edges as templates for the one-dimensional epitaxial growth of hBN domains [18].

2. SYNTHESIS OF TWO-DIMENSIONAL HYBRID-DOMAIN SUPERLATTICES

The discovery of coherent and sharp in-plane boundaries between graphene and hBN domains [13] practically sparked numerous investigations into the synthesis of interfaces between 2D materials, domain structures, along with the

detailed characterization of the synthesis process and their electronic properties. The reason for these new investigations is the implied promise that new 2D materials and combinations thereof could lead to new physical phenomena, to new ways of synthesizing such nanomaterials, and also to new ways of controlling some of their properties so as to facilitate the observation of new phenomena and their applications. Indeed, at least as far as the hybrid-domain monolayer are concerned, they have interesting electronic properties associated with the interfaces between graphene and boron nitride, such as the opening of a controllable bandgap [14, 17, 19], controllable magnetism [20], unique thermal transport properties [21], robust half-metallic behaviour without applying electric fields [14, 17], and interfacial electronic states that are analogous to those observed in oxide heterostructures [22]. Access to these properties depends on the ability to synthesize hybrid domains, hence on methods for controlling the formation of graphene-boron nitride interfaces within a single atomic layer.

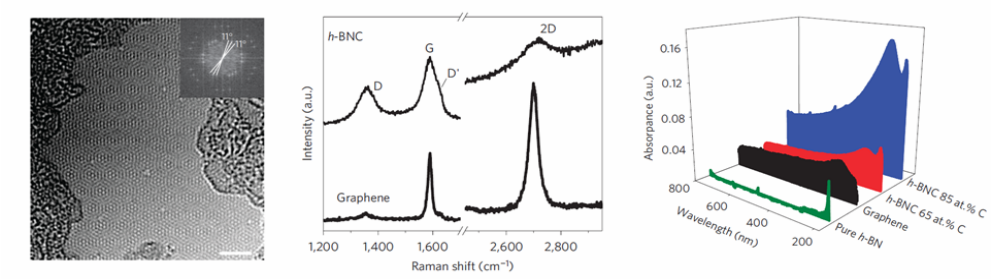

Fig. 1 – Evidence of graphene-BN domain boundaries from Ci *et al*. [13]. Left: high resolution transmission electron images of moiré pattern of hybrid domain graphene-hBN structure. Middle: Raman spectrum of a hybridized domain structure in comparison to that of graphene. Right: adsorption spectra of pure hBN, pure graphene, and hybridized domain with varying levels of carbon (adapted from Ref. 13, with permission from Nature Publishing Group).

The synthesis approach of Ci *et al*. was practically chemical vapour deposition (CVD) performed on copper, and using methane and ammonia borane as simultaneous sources of carbon and hBN, respectively. The atomic percentage of C was controlled in a desired range, while the B-to-N ratio was always unity. Subsequent lithographic patterning was performed, along with a suite of characterization experiments; data from some of these experiments is shown in Fig. 1. By combining in-plane domains of carbon and hBN, a whole range of electronic transport properties could be engineered. It is therefore not surprising that subsequent work has focused on closer control of the interfaces and domains widths. It is not the intent to review here all the subsequent work on the formation and characterization of domains and interfaces between graphene and boron nitride; mentioning a couple of key examples of engineering graphene-hBN interfaces would suffice for the purpose of illustrating the degree of control that is currently achievable in experiments.

In recent experiments, Sutter *et al*. [12] in Fig. 2, as well as Han *et al*. [23], have shown that in-plane monolayer domains of graphene and hBN can form both diffuse interfaces as well as sharp ones, depending on how one controls the amount of carbon adatoms remaining on the surface during the CVD growth of hBN. In both experiments, the formation of the interfaces was carefully controlled and characterized. This indicates that large scale production of in-plane superlattices with alternate domains of different atomic/molecular types should not be too far away.

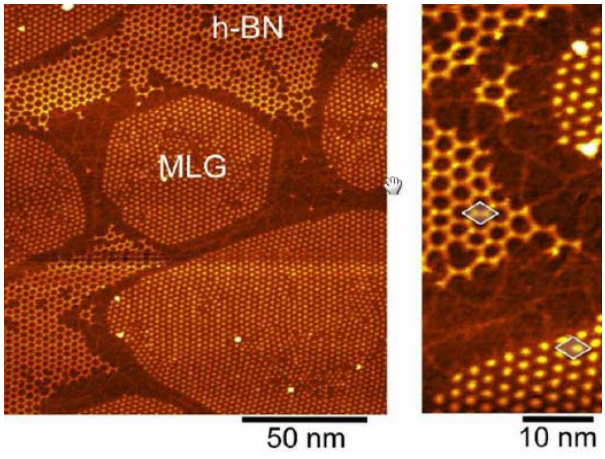

Fig. 2 – Graphene and h-BN domains on Ru(0001), identified by the distinct moiré patterns in scanning tunnelling microscopy experiments. In the region between the graphene and hBN domains, any moiré patterns are absent: in that region, the substrate is covered with a 2D C-B-N alloy (from Ref. [12], with permission from American Chemical Society).

3. MECHANICAL STABILITY OF DOMAIN BOUNDARIES

The discovery of graphene [24] has been followed by observations of a variety of other 2D monolayer crystals [25, 26], in particular, hBN. The near-match of the lattice parameters of graphene and BN has triggered theoretical studies of combined graphene-BN ribbons [17, 27, 28], and more recently domain-hybridized graphene-BN monolayers [13]. Meanwhile, still-hypothetical silicon carbide nanoribbons have also been attracting growing interest [29–31], motivated by the synthesis of silicon carbide nanotubes [32]. While these studies have been focused on the electronic and magnetic properties, rigorous investigations on their structural and mechanical properties have followed [14, 33, 34], and we draw our review of mechanical properties from these studies, in particular from that by Jun *et al*. [14]. In order to tailor the physical and chemical properties pf graphene-hBN domains for future nanoscale device applications, there is a need to understand their structural and mechanical properties, and in particular their elastic stability.

In this section, we review the fundamental elastic properties and deformation behaviors of the pristine edges in boron nitride and silicon carbide monolayer nanoribbons (BNNR and SiCNR respectively), and of the domain boundaries in freestanding domain hybridized graphene-BN monolayer superlattices (CBNSL). Edge and boundary energies have been reported for certain cases [13], but these can only provide a certain amount of knowledge of chemical stability. To understand their mechanical stability and deformation behaviour, we start by determining the edge stresses for nanoribbons (or boundary, in the case of heterophase domains). We present below our first-principles density functional theory (DFT) calculations of edge (boundary) energy and stress for nanoribbons (domain superlattices), and we analyze the results in comparison with previous reports on graphene nanoribbons (GNR) [33–36].

Similar to the interface energy and stress in 3D crystals [37, 38], the boundary energy quantifies the cost to form a new boundary separating different domains (*i.e.*, graphene and BN domains), while boundary stress characterizes the work necessary to stretch a pre-existing boundary along the boundary direction. By definition, the boundary energy is the total excess energy per unit length (with respect to individual bulk 2D crystals), possessed by all atoms in the vicinity of the boundary. On the other hand, the boundary stress characterizes the work per unit boundary length needed to deform a boundary by elastically straining both monolayer domains by the same amount of strain along the boundary direction [38]. The relationship between boundary energy σ and boundary stress h is similar to the Shuttleworth relation between surface energy and surface stress [39], and is written as

$$h = \sigma + \frac{\mathrm{d}\sigma}{\mathrm{d}e},$$

where the stress h and the strain e are scalar quantities since we only consider one-dimensional deformation along the straight boundary line. We note that e is the elastic strain applied to the boundary across which the lattices of both 2D crystal phases are already matched. The above equation also applies to the relation between edge energy and edge stress for nanoribbons.

Boundary energies are calculated from the total energy difference between model systems with and without boundary, and boundary stresses are obtained by numerical differentiation of the boundary energy calculated at a series of strain values within the elastic range. The total-energy calculation is thus the main numerical procedure in this work. Total-energy DFT calculations were performed using the SIESTA code [40] based on local density approximation (LDA), with pseudopotentials and basis set functions similar to those used in earlier work by Jun [34]. An energy cutoff of 250 Ry was set for the real-space integrations. The atomic positions were relaxed via conjugate gradient procedure with force tolerances set to 0.02 eV/Å. We have first obtained the lattice constants of perfect graphene (2.468 Å, hBN (2.492 Å), and SiC (3.081 Å) monolayers.

We considered two types of boundary models, armchair and zigzag, depending on the way in which the two domains face each other at the C-BN boundary. Experimental fabrication of domain-hybridized graphene-BN monolayers revealed that the local atomic structure of heterophase boundaries is either armchair or zigzag [13]. Two examples of supercells with domain boundaries for armchair and zigzag graphene-BN superlattices are shown in Fig. 3. We have constructed various supercell widths of up to ~80 Å for armchair and up to ~86 Å for zigzag models. The numbers in our naming scheme follow the convention for nanoribbons, and thus give the supercell width as the number of dimers in armchair models, or as the number of zigzag lines in zigzag supercells. In out-of-plane direction of all supercells, we insert a vacuum spacing of 15 Å to the interactions between periodic images; a 15 Å vacuum spacing is also introduced along one in-plane direction for nanoribbon models. We kept the same number of dimer (or zigzag) lines for the graphene and BN domains in a supercell, however, it is expected that varying independently the widths of the two domains will provide a valuable additional degree of control.

For the CBN superlattice models, we computed the boundary energy as

$$\sigma = \frac{E_T - N_C E_C - N_{BN} E_{BN}}{2L},$$

where E_T is the total energy of a model supercell which has N_C number of carbon atoms and N_{BN} number of boron-nitrogen pairs. L is the length of the boundary, E_C is the energy per atom in perfect graphene, and E_{BN} is the energy per B-N pair in perfect BN monolayer. Without the term of E_{BN} (E_C), the excess energy σ becomes the edge energy of a graphene (boron nitride) nanoribbon. To calculate the energy of one carbon atom in perfect graphene, or one BN or SiC pair in perfect hBN or perfect SiC, respectively, we employed their fully periodic 4-atom unit cells, and chose 16×16×1 (24×24×1 for SiC) *k*-point mesh by the Monkhorst-Pack scheme. This *k*-point sampling was scaled according to the size of supercells. Typical nanoribbon models having pristine armchair and zigzag edges are also shown in Fig. 3. Elastic properties of graphene edges have also been reported in other works [33–36].

Table 1

Boundary energy and stresses for several nanoribbons and domain boundaries

	Boundary energy (eV/Å)		Boundary stress (eV/Å)	
GNR	1.190 (a)	1.490 (z)	–1.355 (a)	–0.743 (z)
BNNR	0.927 (a)	1.453 (z)	–0.552 (a)	+0.323 (z)
SiCNR	0.885 (a)	0.962 (z)	–0.207 (a)	–0.507 (z)
CBNSL	0.228 (a)	0.293 (z)	–0.167 (a)	+0.027 (z)

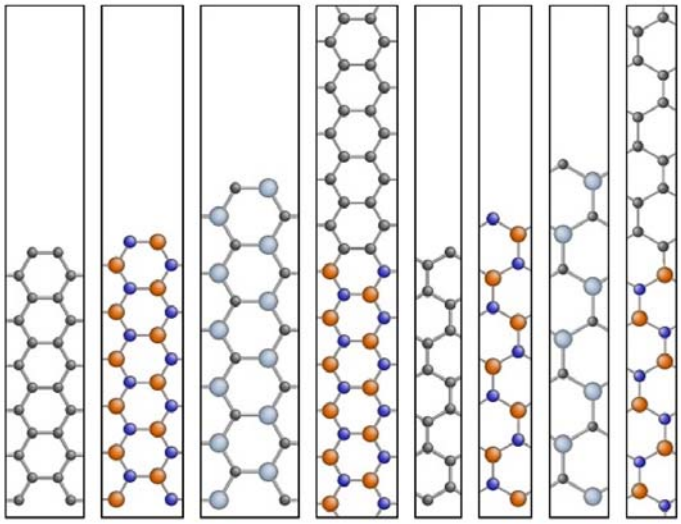

Fig. 3 – Typical supercell models for nanoribbons and domain superlattices before relaxation (from left to right): armchair graphene nanoribbon (aGNR12), armchair BN nanoribbon (aBNNR12), armchair SiC nanoribbon (aSiCNR12), armchair grapne-BN superlattice (aCBNSL22), zigzag graphene nanoribbon (zGNR07), zigzag BN nanoribbon (zBNNR07), zigzag SiC nanoribbon (zSiCNR07), and zigzag graphene-BN superlattice (zCBNSL12) (reproduced from Ref. [14] with permission of American Physical Society).

In Fig. 4, we present our numerical results of edge (boundary) stress for all models with respect to the width of ribbon (stripe). This is because the boundary and edge energies show little dependence on the widths. The width-averaged edge (and boundary) energy and stress values are summarized in Table 1. From plane-wave based DFT calculations, Huang *et al*. [36] have reported graphene edge energies of ~1.00 and ~1.40 eV/Å for armchair and zigzag edges, respectively, which are somewhat smaller than our values (1.190 and 1.490 eV/Å respectively). Plane-wave based DFT calculations have also lead to a value of 0.29 eV/Å zigzag boundary energy in graphene-BN domain superlattices [13], which agrees well with our average value of 0.293 eV/Å.

For both armchair and zigzag cases, boundary energies are substantially lower than edge energies of pristine graphene, BN, and SiC nanoribbons due to the absence of dangling bonds at the boundary. It is known that armchair edge energy of graphene nanoribbon is lower than its zigzag counterpart. We note the same trend in other ribbon edges and graphene-BN boundaries. However, the physical origins of these lower armchair energies are somewhat different. The difference of edge energy between armchair and zigzag GNRs is approximately 0.300 eV/ Å. This relatively large difference comes from the fact that along armchair edge the edge-parallel C-C bond is relaxed to a shorter length than that of interior C-C bond,

due to the strong pair of the *sp* hybridization, which results in the healing of dangling-bond nature of the armchair edge carbon dimers [41]. In contrast, the zigzag edge does not change much its atomic structure after relaxation, and thus it does not substantially reduce the high edge energy caused by dangling bonds.

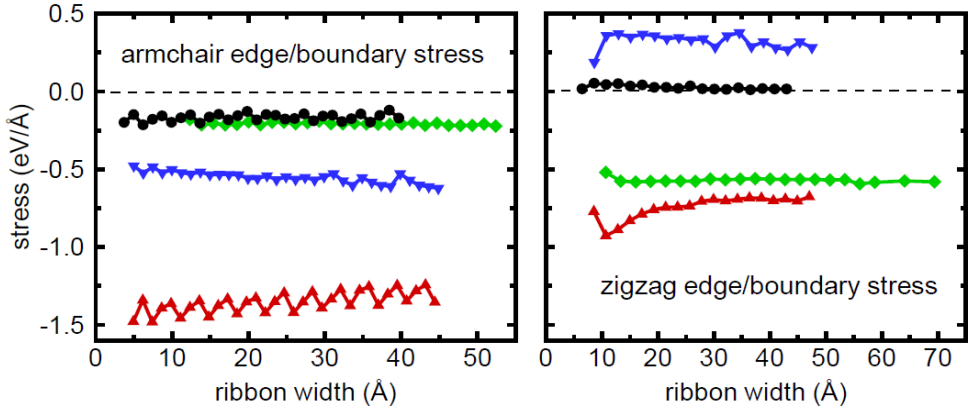

Fig. 4 – Edge/domain-boundary energy and stress as functions of the nanoribbon/stripe width (reproduced from Ref. [14] with permission from American Physical Society).

The edge energy difference between armchair and zigzag becomes even larger for BNNRs. After relaxation, the armchair edge in graphene still maintains the hexagonal lattice structure fairly well in spite of the shortened C-C bond. However, in the armchair BNNR (SiCNR as well), the edge hexagons are distorted so significantly that the original hexagonal symmetry is broken (we show such distorted hexagons of armchair BN and SiC ribbons in a subsequent figure, when we discuss edge stresses). Such distortion provides the armchair BN edge with the opportunity to reduce energy by further relaxing its edge structure while such relaxation is not present for zigzag BN edges. On the other hand, the difference of edge energies between armchair and zigzag SiCNRs is not as large as GNRs and BNNRs. The originally edge-parallel Si-C bond was shortened by 4.93% while those of GNR and BNNR were 12.20% and 9.91% shortened. We therefore believe that the dangling-bond healing effect is less significant in armchair SiCNR edge and that the distortion of edge hexagons is the main source of lowering the armchair edge energy of SiCNR. The boundary energy difference between armchair and zigzag boundaries is remarkably smaller, 0.065 eV/Å, than the above two cases of graphene and BN edges. In our superlattice models of both armchair and zigzag boundaries, we could not observe any obvious change in lattice structure and atomic positions after relaxation, even in the vicinity of boundary. Therefore, the absence of dangling bonds is the key physical reason for which the armchair and zigzag boundaries have similar energies in CBNSL.

The panels of Fig. 4 show our results of edge (boundary) stress calculations for armchair and zigzag edges (boundaries). Edge (boundary) stresses are seen to depend more sensitively on the width of the ribbon (stripe) than the edge (boundary) energies. The average stress values are given in Table 1. Our edge stress values for GNR are comparable with those obtained using plane-wave basis codes [36]. We note that the edge stress of pristine zBNNR is positive. However, all other edges have negative stress values. This means that they are in compression and that their edges tend to ripple whenever they are free to deform at a finite temperature [33]. In contrast, the bare zigzag edge of BNNR is in tension and tends to shorten relative to the interior domain. Therefore, rippling is likely to take place at the interior domain of BN ribbon, away from the zigzag edge, while the edge itself will stay straight.

There are two different types of pristine zigzag edges of BNNR, B-terminated and N-terminated edges. If one edge side is B-ended then the other side is N-ended. Since the charge densities of N- and B-terminated edges are substantially different, their edge energies and edge stresses are quite different as well, and consequently these two pristine zigzag edges may deform in distinct ways. The edge energy and stress presented for zBNNR in Table 1 are the average values between these two zigzag edge types. This argument also applies to the zigzag edge of SiCNR and to the zigzag boundary of CBN superlattice.

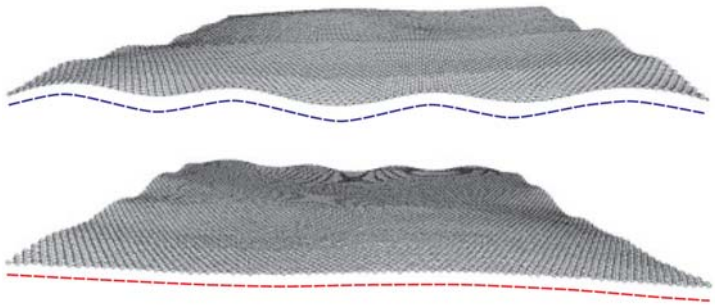

Fig. 5 – Deformation behaviors of (top) C-terminated and (bottom) Si-terminated zigzag edges in a SiC monolayer, simulated via constant temperature molecular dynamics. Dash lines are guides to the eye (reproduced from Ref. [14] with permission from American Physical Society).

To verify the distinct behaviours of zigzag edges with different terminations, we calculated also the edge stresses of both sides separately. Since DFT approaches are unable to yield separate edge energies, we performed energy minimizations and classical molecular dynamics simulations using the Tersoff potential [42] for Si-C systems. The edge energies and stresses calculated using the Tersoff potential are virtually independent of the ribbon width. The edge energy of C-side (Si-side) zigzag edge is 0.559 (0.596) eV/Å, and their average value is 0.577 eV/ Å. The edge stress of C-side (Si-side) zigzag edge is – 0.587 (– 0.222) eV/Å while the average

value of zigzag edge stress is –0.406 eV/Å. Although this average edge stress value is somewhat lower than that obtained by DFT calculations (– 0.570 eV/Å), our empirical potential calculations clearly evidence that the C-side zigzag edge has a higher compressive edge stress value than Si-side edge. This implies that the C edge has a higher rippling tendency than the Si edge, which we have also confirmed by constant-temperature molecular dynamics simulations at 300 K. A snapshot of a large SiC monolayer with 18 718 atoms (dimensions of 320.22 Å × 240.34 Å) is shown in the bottom inset of Figure 5, which verifies the more frequent rippling (higher compressive stress) of the C-ended zigzag edge.

One of our findings is that the boundary stresses in graphene-BN superlattices are significantly lower than the edge stresses of the GNR and BNNR. Our results of – 0.167 eV/Å for armchair and + 0.027 eV/Å for zigzag boundaries are even lower than the edge stresses of hydrogen-passivated graphene edges, – 0.35 eV/Å (armchair) and + 0.13 eV/Å (zigzag) reported earlier [36]. This strongly suggests that C-BN superlattice boundaries experience very low stress and therefore they do not have a tendency to ripple within a hybrid domain heterostructure. We predict that the existence of domain boundaries in graphene-BN monolayer structures will cause neither structural change nor severe deformation.

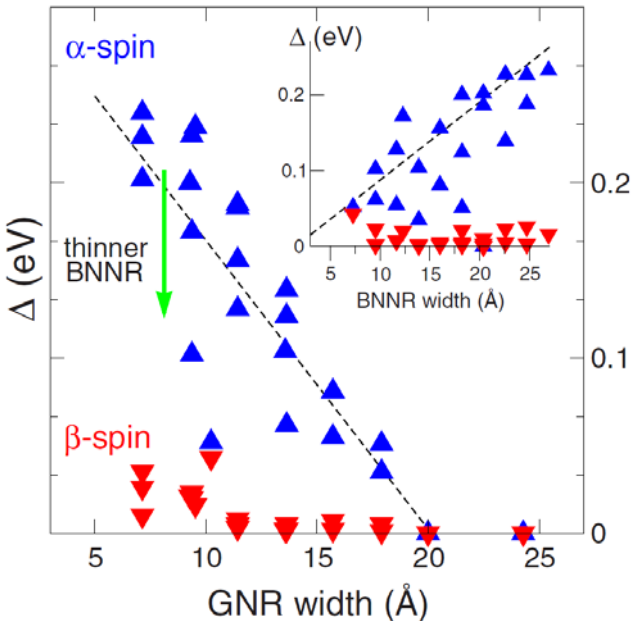

Fig. 6 – Bandgaps for the spin-up component (blue triangles) and spin-down component (red triangle) as functions of the stripe width in the antiferomagnetic ground state for the graphene-hBN superlattices. The green arrow shows the dependence of the spin-up bandgap on the width of the BN strip (from Ref. [17], with permission of American Physical Society).

4. ELECTRONIC PROPERTIES

The key property of these superlattices appears for those with zigzag domain boundaries, and consists in different bandstructures for the two spin components. Figure 6, from a recent report of Pruneda [17], shows the variation of the bandgap for the two spin components. If the graphene domains are large, then the (expected) semimetallic behaviour is recovered. In the other limit, in which the graphene domains are narrow, the antiferromagnetic state becomes unstable and, with it, the system becomes nonmagnetic and insulating. As seen in Fig. 6, there is a range of domain widths in which the system is metallic in the spin-down component and semiconducting in the spin-up component. Based on DFT calculations, Pruneda has provided an explanation for the half-metallicity of the hybrid-domain superlattices [17]: the magnetic properties of the stripe edges of graphene, coupled with the polarity of the BN stripes lead to asymmetries in the spin screening, thereby inducing an electronic rearrangement ("reconstruction") at the domain edges. As seen in Fig. 7, the bandgap in the spin-up component can be as high as 0.3 eV while the other spin component can be metallic. This finding is anticipated to lead to very interesting phenomena at the 1D domain interfaces, phenomena that may include even superconductivity (by analogy with 2D interfaces in perovskites). Furthermore, electronic conduction is expected to be highly anisotropic, especially within the hBN domains.

Another interesting property of the graphene-BN domain superlattice, is the very large Siebeck coefficient that can be achieved [43]. This coefficient is crucial in characterizing the efficiency of thermoelectric conversion and the primary indicator of a large thermoelectric figure of merit. While the physical origins of this increase in the Siebeck coefficient is not fully understood, the coefficient has been computed for a wide range of graphene-BN superlattices and its dependence of the stripe width is known. The key to achieve it is a low width for the hBN, which seems to be the factor that has most effect regarding the deviation of the Siebeck coefficient from the value corresponding to pure graphene.

Structurally, the domain boundaries (while not very reactive in a chemical sense) have shown promise as templates for 1D nanostructures (essentially wires or very small atomic clusters) grown on top of the graphene-BN superlattices. In a recent work [44], Haldar and coworkers have calculated the diffusion barriers of Fe atoms on such superlattices. They have shown that iron atoms diffuse much more easily on BN than on graphene, and that during only a few picoseconds at room temperature they diffuse across the C-N domain boundary to get trapped at the C-B boundaries. Furthermore, Haldar et al. showed that the magnetic exchange coupling between Fe clusters at C-B domain boundaries varies nonmonotonically as a function of the hBN stripe width. These superlattices can therefore act as templates for the spontaneous formation of magnetic nanostructures at specific interfaces.

Lastly, we mention that Bristowe *et al*. [45] have predicted half-metallic 1D interfaces between two insulating domains, made, for example, several II–VI, III–V, and IV–IV compounds, whose stable bulk phase is wurtzite but which may assume a highly planar phases in atomically thin films. These authors show, expectedly, that 1D domain boundaries in these insulator-insulator superlattices are polar, having a net excess charge determined from using the formal valence charges of the atomic species involved, irrespective of the predominant covalent character of the bonding in these materials; furthermore, they rationalize such finding by analysing the topology of the formal polarization lattice in the parent bulk materials. DFT calculations similar to those in Ref. 17 show an electronic compensation mechanism due to a Zener-like charge transfer between interfaces of opposite polarity. The emergence of one-dimensional electron and hole gases is predicted [45].

5. CONCLUSIONS

In conclusion, we have reviewed recent reports on the mechanical and electronic properties of hybrid domain superlattices. In terms of mechanical properties, we have shown that a key quantity characterizing the stability and "flatness" of a domain boundary is the domain boundary stress. Calculating the stresses is rather straight-forward, with rapid meaningful conclusions for the stability of the domain edges. We have found that the C-BN boundaries experience very little stress and thus the existence of such domain boundaries will cause neither structural change nor severe deformation in C-BN superlattices. The oscillating values of armchair boundary stress indicate that armchair CBNSL may be semiconducting. Furthermore, it is shown that the broken hexagonal symmetry of armchair BN and SiC ribbons results in their irregularly oscillating stress values as functions of ribbon width. Lastly, we have shown that two types of zigzag edges in SiC nanoribbon undergo distinctly different deformations.

In terms of electronic properties, three major ones stand out, all of which dependent on the size of the domain-widths: (a) half metallicity, (b) edge magnetism, and (c) giant Siebeck coefficient. These properties pertain to graphene-hBN superlattices, although it is expected that conditions favorable to their occurrence can be met in superlattices made of other materials as well [45]. These exotic properties, along with their immediate "control knobs" (domain-widths, either intrinsic or possibly strain controlled), are evolving into a new niche in the field of 2-D materials. Fundamental and technological advances based on these properties are expected to rapidly take off in the near future, and we expect than an enhanced understanding of the transport at the interface will lead to game-changing paradigms as far as the miniaturization of the nanoelectronic devices is concerned.

Acknowledgements. I would like to thank Dr. R. Catalin Picu for the kind invitation to contribute this article. I am indebted to my co-authors of Ref. [14], F. Meng, X. Li and Prof. S. Jun, most of which has been included, with permission from American Physical Society, in the mechanical properties section of this review.

Received on March 24, 2016

REFERENCES

1. LI, X., CAI, W., AN, J., KIM, S., NAH, J., YANG, D., PINER, R., VELAMAKANNI, A., JUNG, I., TUTUC, E., BANERJEE, S.K., COLOMBO, L., RUOFF, R.S., *Large-Area Synthesis of High-Quality and Uniform Graphene Films on Copper Foils*, Science, **324**, pp. 1312–1314, 2009.
2. BAE, S., KIM, H., LEE, Y., XU, X., PARK, J.-S., ZHENG, Y., BALAKRISHNAN, J., LEI, T., KIM, H.R., SONG, Y.I., KIM, Y.-J., KIM, K.S., OZYILMAZ, B., AHN, J.-H., HONG, B.H., IIJIMA, S., *Roll-to-roll production of 30-inch graphene films for transparent electrodes*, Nature Nanotechnology, **5**, pp. 574–578, 2010.
3. SUN, Z., YAN, Z., YAO, J., BEITLER, E., ZHU, Y., TOUR, J.M., *Growth of graphene from solid carbon sources*, Nature, **468**, pp. 549–552, 2010.
4. REINA, A., JIA, X., HO, J., NEZICH, D., SON, H., BULOVIC, V., DRESSELHAUS, M.S., KONG, J., *Large Area, Few-Layer Graphene Films on Arbitrary Substrates by Chemical Vapor Deposition*, Nano Letters, **9**, pp. 30–35, 2009.
5. LEE, K.H., SHIN, H.-J., LEE, J., LEE, I.-Y., KIM, G.-H., CHOI, J.-Y., KIM, S.-W., *Large-Scale Synthesis of High-Quality Hexagonal Boron Nitride Nanosheets for Large-Area Graphene Electronics*, Nano Letters, **12**, pp. 714–718, 2012.
6. SONG, L., CI, L., LU, H., SOROKIN, P.B., JIN, C., NI, J., KVASHNIN, A.G., KVASHNIN, D.G., LOU, J., YAKOBSON, B.I., AJAYAN, P.M., *Large Scale Growth and Characterization of Atomic Hexagonal Boron Nitride Layers*, Nano Letters, **10**, pp. 3209–3215, 2010.
7. YANG, W., CHEN, G., SHI, Z., LIU, C.-C., ZHANG, L., XIE, G., CHENG, M., WANG, D., YANG, R., SHI, D., WATANABE, K., TANIGUCHI, T., YAO, Y., ZHANG, Y., ZHANG, G., *Epitaxial growth of single-domain graphene on hexagonal boron nitride*, Nature Materials, **12**, pp. 792–797, 2013.
8. XUE, J., SANCHEZ-YAMAGISHI, J., BULMASH, D., JACQUOD, P., DESHPANDE, A., WATANABE, K., TANIGUCHI, T., JARILLO-HERRERO, P., LEROY, B.J., *Scanning tunnelling microscopy and spectroscopy of ultra-flat graphene on hexagonal boron nitride*, Nature Materials, **10**, pp. 282–285, 2011.
9. WANG, M., JANG, S.K., JANG, W.-J., KIM, M., PARK, S.-Y., KIM, S.-W., KAHNG, S.-J., CHOI, J.-Y., RUOFF, R.S., SONG, Y.J., LEE, S., *A Platform for Large-Scale Graphene Electronics - CVD Growth of Single-Layer Graphene on CVD-Grown Hexagonal Boron Nitride*, Advanced Materials, **25**, pp. 2746–2752, 2013.
10. LIU, Z., SONG, L., ZHAO, S., HUANG, J., MA, L., ZHANG, J., LOU, J., AJAYAN, P.M., *Direct Growth of Graphene/Hexagonal Boron Nitride Stacked Layers*, Nano Letters, **11**, pp. 2032–2037, 2011.
11. RAMASUBRAMANIAM, A., NAVEH, D., TOWE, E., *Tunable Band Gaps in Bilayer Graphene-BN Heterostructures*, Nano Letters, **11**, pp. 1070–1075, 2011.
12. SUTTER, P., CORTES, R., LAHIRI, J., SUTTER, E., *Interface Formation in Monolayer Graphene-Boron Nitride Heterostructures*, Nano Letters, **12**, pp. 4869–4874, 2012.
13. CI, L., SONG, L., JIN, C., JARIWALA, D., WU, D., LI, Y., SRIVASTAVA, A., WANG, Z.F., STORR, K., BALICAS, L., LIU, F., AJAYAN, P.M., *Atomic layers of hybridized boron nitride and graphene domains*, Nature Materials, **9**, pp. 430–435, 2010.

14. JUN, S., LI, X., MENG, F., CIOBANU, C.V., *Elastic properties of edges in BN and SiC nanoribbons and of boundaries in C-BN superlattices: A density functional theory study*, Physical Review B, **83**, pp. 153407, 2011.
15. HAN, M.Y., OZYILMAZ, B., ZHANG, Y.B., KIM, P., *Energy band-gap engineering of graphene nanoribbons*, Phys. Rev. Lett., **98**, pp. 206805, 2007.
16. SON, Y.-W., COHEN, M.L., LOUIE, S.G., *Energy gaps in graphene nanoribbons*, Phys. Rev. Lett., **97**, pp. 216803, 2006.
17. PRUNEDA, J.M., *Origin of half-semimetallicity induced at interfaces of C-BN heterostructures*, Physical Review B, **81**, pp. 161409, 2010.
18. LIU, L., PARK, J., SIEGEL, D.A., MCCARTY, K.F., CLARK, K.W., DENG, W., BASILE, L., IDROBO, J.C., LI, A.P., GU, G., *Heteroepitaxial Growth of Two-Dimensional Hexagonal Boron Nitride Templated by Graphene Edges*, Science, **343**, pp. 163–167, 2014.
19. HE, J., CHEN, K.-Q., FAN, Z.-Q., TANG, L.-M., HU, W.P., *Transition from insulator to metal induced by hybridized connection of graphene and boron nitride nanoribbons*, Applied Physics Letters, **97**, pp. 193305, 2010.
20. RAMASUBRAMANIAM, A., NAVEH, D., *Carrier-induced antiferromagnet of graphene islands embedded in hexagonal boron nitride*, Physical Review B, **84**, pp. 075405, 2011.
21. JIANG, J.-W., WANG, J.-S., WANG, B.-S., *Minimum thermal conductance in graphene and boron nitride superlattice*, Applied Physics Letters, **99**, pp. 043109, 2011.
22. OHTOMO, A., HWANG, H.Y., *A high-mobility electron gas at the LaAlO3/SrTiO3 heterointerface* (vol. 427, p. 423, 2004), Nature, **441**, pp. 120–120, 2006.
23. HAN, G.H., RODRIGUEZ-MANZO, J.A., LEE, C.W., KYBERT, N.J., LERNER, M.B., QI, Z.J., DATTOLI, E.N., RAPPE, A.M., DRNDIC, M., JOHNSON, A.T.C., *Continuous Growth of Hexagonal Graphene and Boron Nitride In-Plane Heterostructures by Atmospheric Pressure Chemical Vapor Deposition*, ACS Nano, **7**, pp. 10129–10138, 2013.
24. NOVOSELOV, K.S., GEIM, A.K., MOROZOV, S.V., JIANG, D., ZHANG, Y., DUBONOS, S.V., GRIGORIEVA, I.V., FIRSOV, A.A., *Electric field effect in atomically thin carbon films*, Science, **306**, pp. 666–669, 2004.
25. NOVOSELOV, K.S., JIANG, D., SCHEDIN, F., BOOTH, T.J., KHOTKEVICH, V.V., MOROZOV, S.V., GEIM, A.K., *Two-dimensional atomic crystals*, Proceedings of the National Academy of Sciences of the United States of America, **102**, pp. 10451–10453, 2005.
26. JIN, C., LIN, F., SUENAGA, K., IIJIMA, S., *Fabrication of a Freestanding Boron Nitride Single Layer and Its Defect Assignments*, Phys. Rev. Lett., **102**, pp. 195505, 2009.
27. DUTTA, S., MANNA, A.K., PATI, S.K., *Intrinsic Half-Metallicity in Modified Graphene Nanoribbons*, Phys. Rev. Lett., **102**, pp. 096601, 2009.
28. DING, Y., WANG, Y., NI, J., *Electronic properties of graphene nanoribbons embedded in boron nitride sheets*, Applied Physics Letters, **95**, pp. 2009.
29. SUN, L., LI, Y., LI, Z., LI, Q., ZHOU, Z., CHEN, Z., YANG, J., HOU, J.G., *Electronic structures of SiC nanoribbons*, Journal of Chemical Physics, **129**, pp. 174114, 2008.
30. LOU, P., LEE, J.Y., *Band Structures of Narrow Zigzag Silicon Carbon Nanoribbons*, Journal of Physical Chemistry C, **113**, pp. 12637–12640, 2009.
31. XU, B., YIN, J., XIA, Y.D., WAN, X.G., LIU, Z.G., *Ferromagnetic and antiferromagnetic properties of the semihydrogenated SiC sheet*, Applied Physics Letters, **96**, pp. 143111, 2010.
32. SUN, X.H., LI, C.P., WONG, W.K., WONG, N.B., LEE, C.S., LEE, S.T., TEO, B.K., *Formation of silicon carbide nanotubes and nanowires via reaction of silicon (from disproportionation of silicon monoxide) with carbon nanotubes*, Journal of the American Chemical Society, **124**, pp. 14464–14471, 2002.
33. SHENOY, V.B., REDDY, C.D., RAMASUBRAMANIAM, A., ZHANG, Y.W., *Edge-Stress-Induced Warping of Graphene Sheets and Nanoribbons*, Phys. Rev. Lett., **101**, pp. 245501, 2008.
34. JUN, S., *Density-functional study of edge stress in graphene*, Physical Review B, **78**, pp. 073405, 2008.

35. BETS, K.V., YAKOBSON, B.I., *Spontaneous Twist and Intrinsic Instabilities of Pristine Graphene Nanoribbons*, Nano Research, **2**, pp. 161–166, 2009.
36. HUANG, B., LIU, M., SU, N., WU, J., DUAN, W., GU, B.-L., LIU, F., *Quantum Manifestations of Graphene Edge Stress and Edge Instability: A First-Principles Study*, Phys. Rev. Lett., **102**, pp. 166404, 2009.
37. CAHN, J.W., LARCHE, F., *SURFACE STRESS AND THE CHEMICAL-EQUILIBRIUM OF SMALL CRYSTALS .2. SOLID PARTICLES EMBEDDED IN A SOLID MATRIX*, Acta Metallurgica, **30**, pp. 51–56, 1982.
38. CAMMARATA, R.C., *SURFACE AND INTERFACE STRESS EFFECTS IN THIN-FILMS*, Progress in Surface Science, **46**, pp. 1–38, 1994.
39. SHUTTLEWORTH, R., *The surface tension of solids*, Proc. Phys. Soc. A, **63**, pp. 444, 1950.
40. SOLER, J.M., ARTACHO, E., GALE, J.D., GARCIA, A., JUNQUERA, J., ORDEJON, P., SANCHEZ-PORTAL, D., *The SIESTA method for ab initio order-N materials simulation*, Journal of Physics-Condensed Matter, **14**, pp. 2745–2779, 2002.
41. OKADA, S., *Energetics of nanoscale graphene ribbons: Edge geometries and electronic structures*, Physical Review B, **77**, pp. 041408, 2008.
42. TERSOFF, J., *MODELING SOLID-STATE CHEMISTRY - INTERATOMIC POTENTIALS FOR MULTICOMPONENT SYSTEMS*, Physical Review B, **39**, pp. 5566–5568, 1989.
43. YOKOMIZO, Y., NAKAMURA, J., *Giant Seebeck coefficient of the graphene/h-BN superlattices*, Applied Physics Letters, **103**, pp. 2013.
44. HALDAR, S., SRIVASTAVA, P., ERIKSSON, O., SEN, P., SANYAL, B., *Designing Fe Nanostructures at Graphene/h-BN Interfaces*, Journal of Physical Chemistry C, **117**, pp. 21763–21771, 2013.
45. BRISTOWE, N.C., STENGEL, M., LITTLEWOOD, P.B., ARTACHO, E., PRUNEDA, J.M., *One-dimensional half-metallic interfaces of two-dimensional honeycomb insulators*, Physical Review B, **88**, pp. 2013.